Supporting Information

Engineering Oxygen Vacancies with Atomically Dispersed WO_x: A Strategy for Superior CO_2 Hydrogenation Performance and Stability on Pd/CeO_2

Mireu Kim[a], Joon Hyun Baik[b,*], Insoo Ro[c,*]

[a] *Department of Chemical and Biomolecular Engineering, Seoul National University of Science and Technology, 01811, Republic of Korea*

[b] *Department of Chemical & Biological Engineering, Sookmyung Women's University, Seoul 04310, Republic of Korea*

[c] *Department of Chemical and Biological Engineering, Korea University, Seoul, 02841 Republic of Korea*

[*] *Corresponding Authors: Prof. J. Baik (joonhyun@sookmyung.ac.kr), and Prof. I. Ro (insooro@korea.ac.kr)*

S1. Kinetic Calculations

Activation energy (kJ/mol) was calculated according to the linearized Arrhenius equation:

$$\ln k = -\frac{E_a}{RT} + \ln A \qquad \text{Eqs. S1}$$

Where: R = gas constant (8.314 J·mol^{-1}·K^{-1})

T = reaction temperature (K)

A = pre-exponential factor

S2. W Surface Density Calculations

W surface density (W atom/nm^2) was calculated according to:

$$\rho_W = \frac{\omega_W \cdot N_A}{SA_W \cdot Z_W} \times 10^{-20} \qquad \text{Eqs. S2}$$

Where: ρ_W = W surface density (W atom/nm^2)

ω_W = W loading (W wt.%)

N_A = Avogadro's number

SA_W = surface area of xWO$_x$-CeO$_2$ (m^2/g)

Z_W = W molar mass (g/mol)

S3. Surface O_v Density Calculations

The surface oxygen vacancy density was calculated for Pd/CeO_2, and $Pd/0.6WO_x$-CeO_2 catalyst using O_2-TPD, BET measurements[17]. The adsorbed molecular $O_{ads.}$ corresponded directly to the molar amount of O_2 adsorbed in the oxygen vacancies. Surface oxygen vacancy density (in sites/nm^2) was calculated according to:

$$\rho_{vac} = \frac{n_{TPD} \cdot N_A}{SA} \qquad \text{Eqs. S3}$$

Where: ρ_{vac} = Surface oxygen vacancy density ($\times 10^{17}$/nm^2)

n_{TPD} = Adsorbed oxygen in $O_{ads.}$ at 150–210 ℃ (mmol/g)

SA = Catalysts surface area (m^2/g)

S4. CO_2 Hydrogenation Reaction Elementary Steps[18]

CO_2 first reacts with coordinatively unsaturated O^{2-} sites in the presence of oxygen vacancies (O_v) to form monodentate or bidentate carbonate species (Eqs. S4).

$$CO_2 + O^* + O_v \leftrightarrow CO_3^* \quad \text{Eqs. S4}$$

Alternatively, CO_2 reacts with surface hydroxyl groups to generate bicarbonate species (Eqs. S5).

$$CO_2 + OH^- \rightarrow HCO_3^- \quad \text{Eqs. S5}$$

The bicarbonate species can then be hydrogenated to form hydrocarboxyl intermediates (Eqs. S6).

$$HCO_3^- + 2H^* \rightarrow COOH^- + H_2O \quad \text{Eqs. S6}$$

Subsequent hydrogenation of carbonate- or bicarbonate-derived species yields formate (HCOO) and methoxy (CH_3O) intermediates (Eqs. S7).

$$CO_3^* + nH_{OH} \leftrightarrow HCOO^*/CH_3O^* + * \quad \text{Eqs. S7}$$

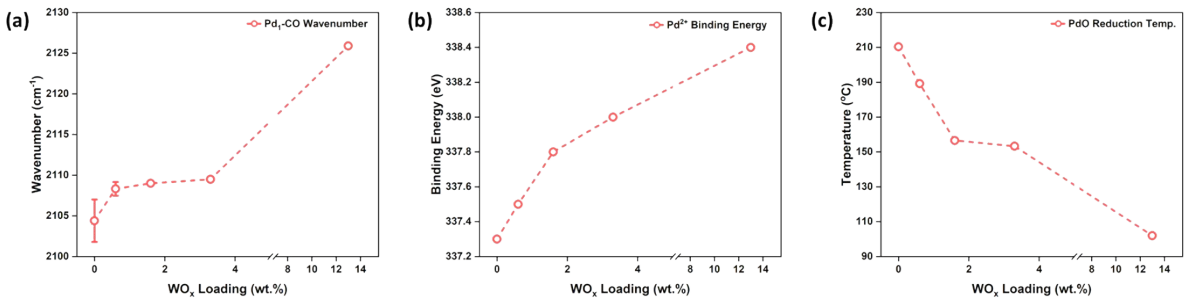

Figure S1. (a) Pd_1–CO stretch position, (b) Pd $3d_{5/2}$ binding energy, and (c) PdO reduction temperature as a function of W loading.

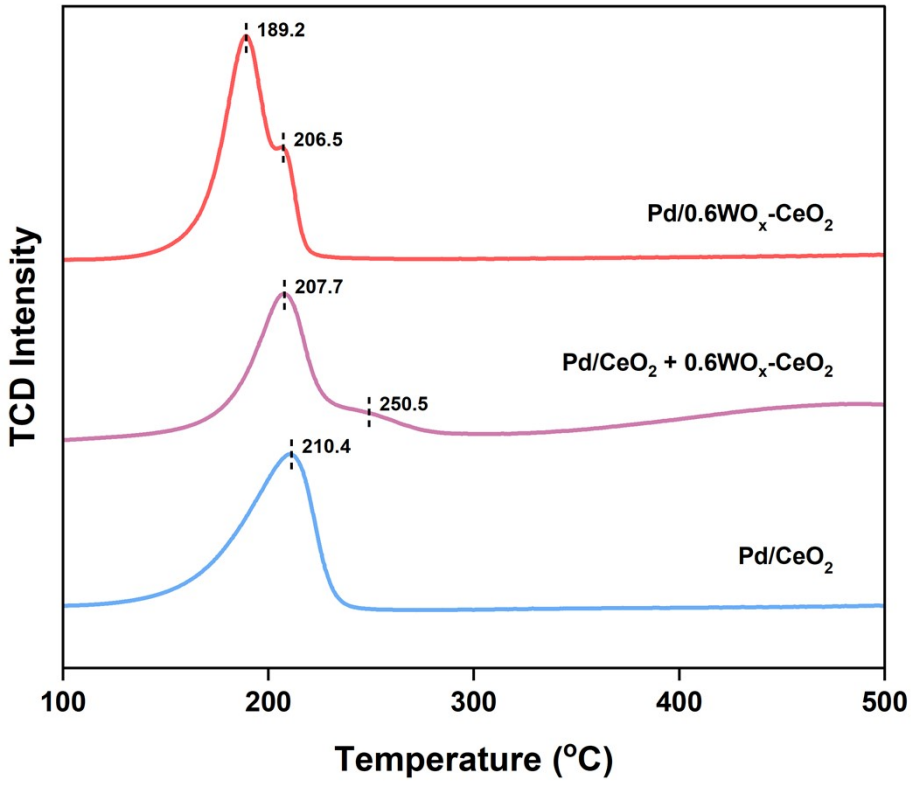

Figure S2. H_2-TPR spectra of synthesized catalysts.

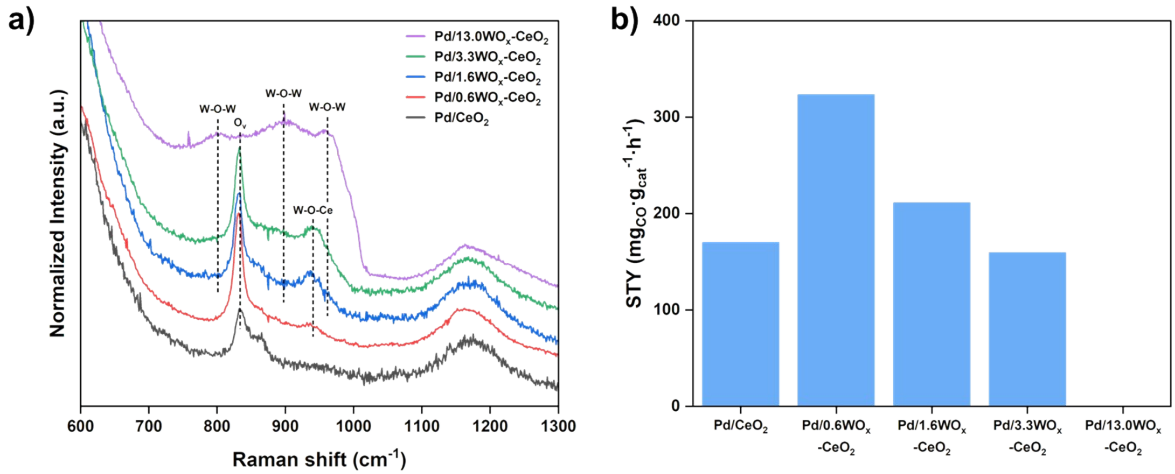

Figure S3. (a) Raman spectra, and (b) Catalytic performance of different W loading. Reaction conditions: 300 °C, 1 bar, 60,000 mL·g_{cat}^{-1}·h^{-1}, H_2/CO_2 = 3

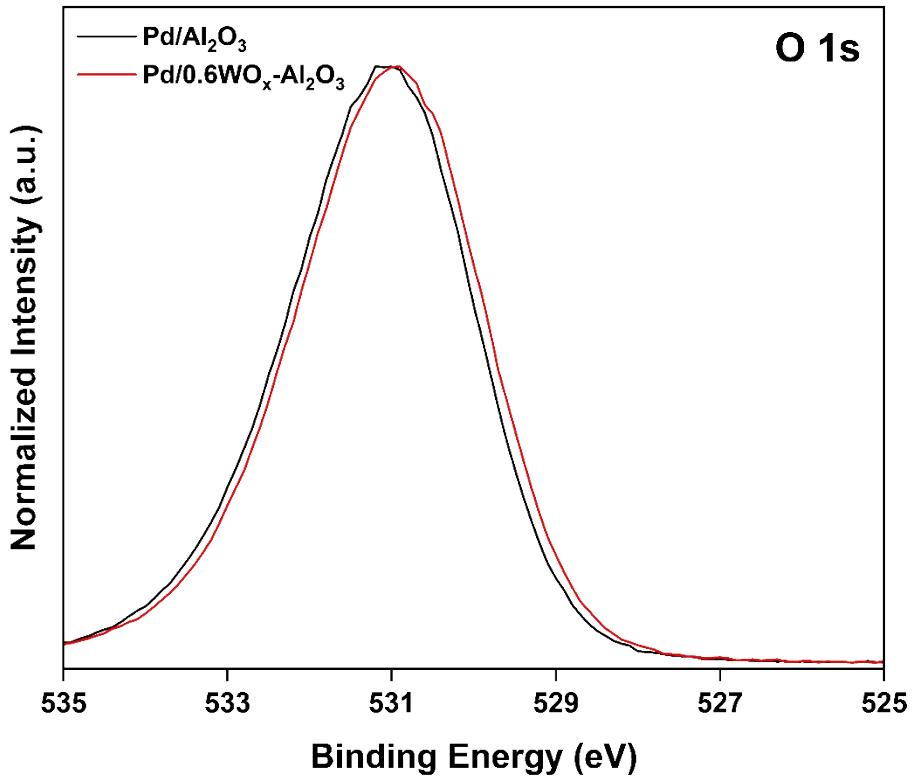

Figure S4. O 1s XPS spectra of Pd/Al_2O_3 and $Pd/0.6WO_x$-Al_2O_3 catalyst after *ex situ* reduction at 200 °C.

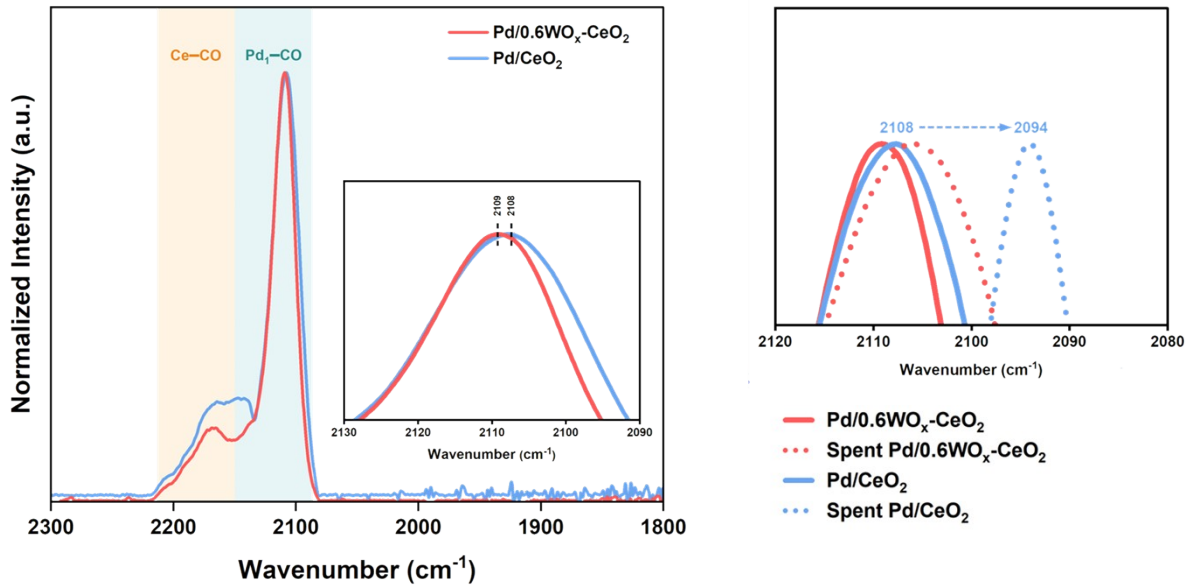

Figure S5. Normalized CO probe molecular DRIFTS spectra of fresh (solid line) and spent (dotted line) catalysts.

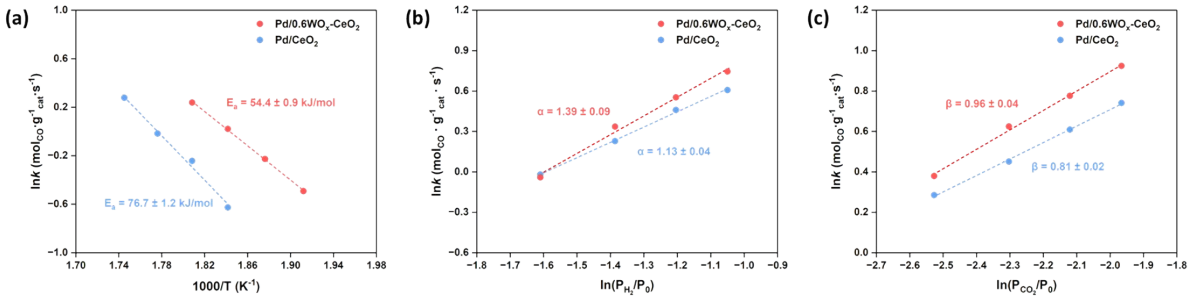

Figure S6. (a) Arrhenius plot of CO formation over Pd/CeO_2 and $Pd/0.6WO_x–CeO_2$ catalysts measured in 10 °C steps at reaction temperatures between 250 and 300 °C. (b) CO formation rate at constant CO_2 pressure as a function of H_2 partial pressure, and (c) CO formation rate at constant H_2 pressure as a function of CO_2 partial pressure for Pd/CeO_2 and $Pd/0.6WO_x–CeO_2$ catalysts measured at 300 °C, 1 bar.

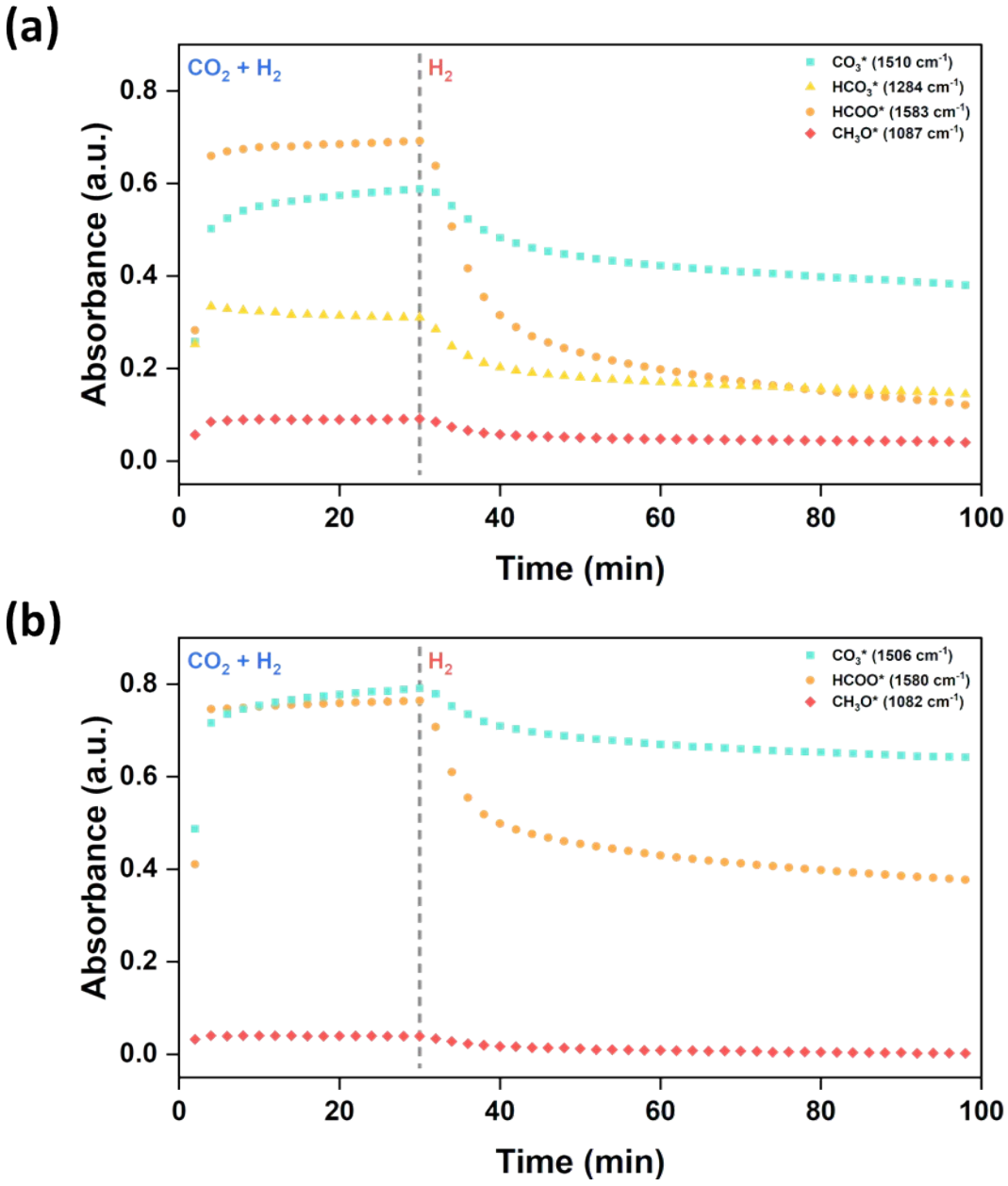

Figure S7. Time and atmospheric composition depend on signal intensities of the typical surface species over (a) Pd/CeO_2 and (b) $Pd/0.6WO_x$-CeO_2. Reaction conditions: 300 °C, 1 bar, 60,000 $mL \cdot g_{cat}^{-1} \cdot h^{-1}$, $H_2/CO_2 = 3$.

Table S1. Support properties with different W loading.

Sample	Surface Area (m^2/g)[a]	W loading (wt.%)[b]	W Surface Density (W atom/nm^2)[c]
Al_2O_3	124.8	–	–
$0.6WO_x$-Al_2O_3	–	1.1	0.30
CeO_2	140.4	–	–
$0.6WO_x$-CeO_2	134.3	0.9	0.22
$1.6WO_x$-CeO_2	123.7	1.7	0.45
$3.3WO_x$-CeO_2	112.8	3.6	1.05
$13.0WO_x$-CeO_2	102.2	14.2	4.52

[a] Catalysts surface area (m^2/g) was calculated from BET results. [b] W loading (wt.%) was determined from ICP-MS results. [c] W surface density (W atom/nm^2) was calculated from surface area and ICP-MS results.

Table S2. Catalyst properties with different W loading.

Catalyst	Surface Area (m^2/g)[a]	Pd loading (wt.%)[b]	Desorbed O_2 from $O_{ads.}$ (mmol/g)[c]	Surface O_v Density ($\times 10^{17}/m^2$)[d]	$O_{ads.}$ Concentration (%)[e]	Ce^{3+} Concentration (%)[e]	W^{5+} Concentration (%)[e]
Pd/CeO_2	126.4	0.25	0.087	4.14	20.6	31.4	–
$Pd/0.6WO_x$-CeO_2	120.1	0.24	0.221	11.08	38.7	33.4	88.0
$Pd/1.6WO_x$-CeO_2	118.3	0.26	0.202	10.28	34.7	27.6	79.8
$Pd/3.3WO_x$-CeO_2	97.0	0.28	0.140	8.65	30.5	25.3	54.5
$Pd/13.0WO_x$-CeO_2	80.3	0.26	0.093	6.89	13.9	19.5	29.1

[a] Catalysts surface area (m^2/g) was calculated from BET results. [b] Pd loading (wt.%) was determined from ICP-MS results. [c] Desorbed O_2 from $O_{ads.}$ (mmol/g) was calculated from O_2-TPD results as the amount of desorbed O_2 below 210 °C. [d] Surface O_v density (site/m^2) was calculated from surface area and desorbed O_2 from $O_{ads.}$ calculated from O_2-TPD results. [e] Surface species concentration (%) was calculated from XPS results.

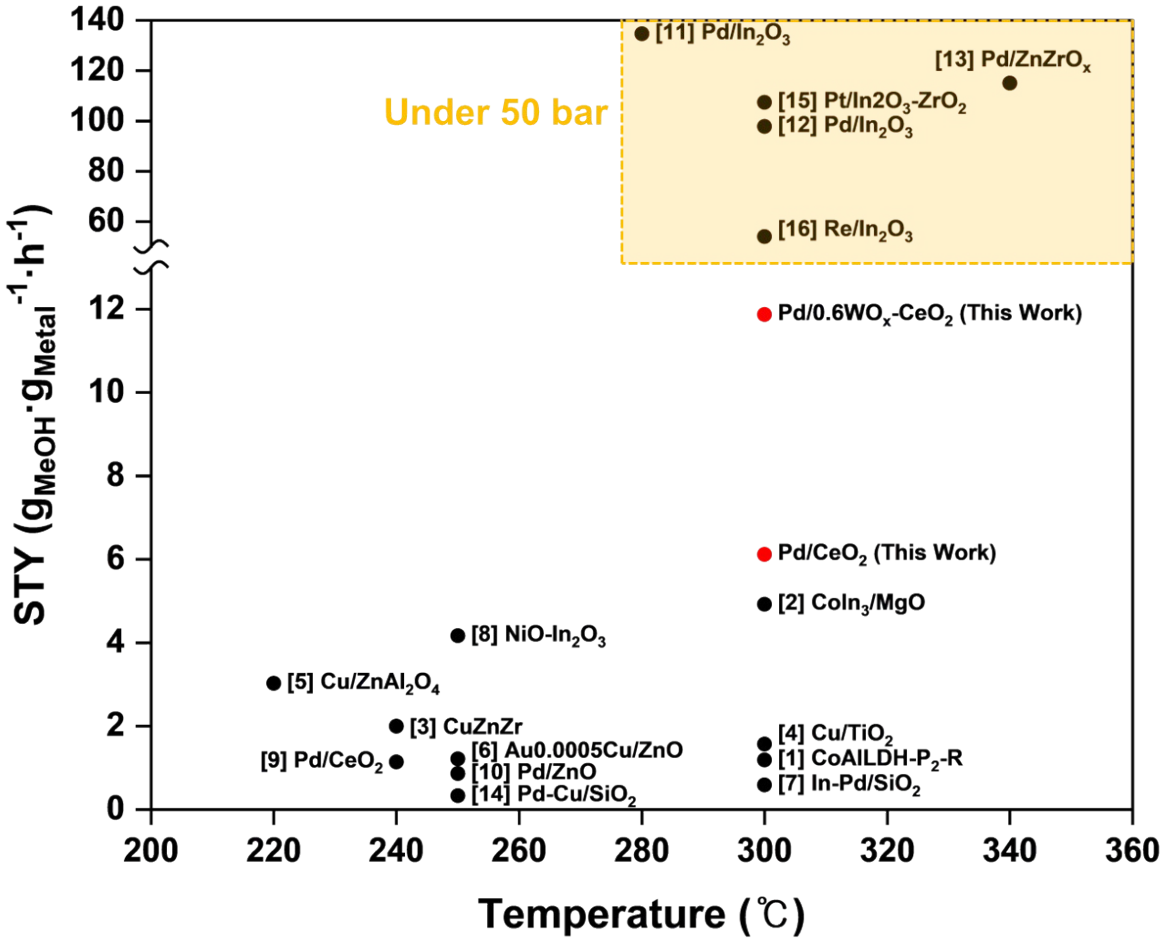

Figure S8. Comparative analysis of the CO_2 hydrogenation catalysts.

Table S3. Summary of the catalytic properties of catalysts for CO_2 hydrogenation.

Catalyst	T (°C)	P (bar)	Metal	Metal loading (wt.%)	STY_{MeOH} ($mg \cdot g_{Metal}^{-1} \cdot h^{-1}$)	Reference
CoAlLDH-P_2-R	300	30	Co	46.7	1.2	1
$CoIn_3$/MgO	300	30	Co	12.5	4.9	2
CuZnZr	240	30	Cu	60.0[a]	2.0	3
Cu/TiO_2	300	40	Cu	5.9	1.6	4
Cu/$ZnAl_2O_4$	220	30	Cu	8.0	3.0	5
Au0.005Cu/ZnO	250	30	Cu	28.0	1.1	6
In-Pd/SiO_2	300	40	In-Pd	–	0.6	7
NiO-In_2O_3	250	30	NiO	6.0	4.2	8
Pd/CeO_2-R	240	30	Pd	2.0	1.2	9
Pd/ZnO	250	20	Pd	1.0	0.9	10
Pd/In_2O_3	280	50	Pd	0.8	134.7	11
Pd-P/In_2O_3	300	50	Pd	0.9	97.8	12
Pd/$ZnZrO_x$	340	50	Pd	0.6	115.0	13
Pd-Cu/SiO_2	250	50	Pd-Cu	15.7	0.3	14
Pt/in_2O_3-ZrO_2	300	50	Pt	0.5	107.4	15
Re/ln_2O_3	300	50	Re	1.0	54.0	16
Pd/0.6WO_x-CeO_2	300	30	Pd	0.2	11.9	This Work
Pd/CeO_2	300	30	Pd	0.2	6.1	This Work

[a] atom %

References

(1) Zhang, H.; Mao, D.; Zhang, J.; Wu, D. Tuning the CO2 hydrogenation path by moderately phosphating the Co-Al catalyst toward methanol synthesis. *Applied Catalysis B: Environmental* **2024**, *340*, 123257.
(2) Zhang, H.; Zhang, J.; Yu, S.; Wu, D. Unique Interatomic Interaction Assisted CoIn Intermetallic Compound for Efficient Hydrogenation of CO2 into Methanol. *ACS Catalysis* **2025**, *15* (6), 4698-4710.
(3) Bonura, G.; Cordaro, M.; Cannilla, C.; Arena, F.; Frusteri, F. The changing nature of the active site of Cu-Zn-Zr catalysts for the CO2 hydrogenation reaction to methanol. *Applied Catalysis B: Environmental* **2014**, *152*, 152-161.
(4) Zhang, C.; Wang, L.; Etim, U. J.; Song, Y.; Gazit, O. M.; Zhong, Z. Oxygen vacancies in Cu/TiO2 boost strong metal-support interaction and CO2 hydrogenation to methanol. *Journal of Catalysis* **2022**, *413*, 284-296.
(5) Song, L.; Wang, H.; Wang, S.; Qu, Z. Dual-site activation of H2 over Cu/ZnAl2O4 boosting CO2 hydrogenation to methanol. *Applied Catalysis B: Environmental* **2023**, *322*, 122137.
(6) Xie, G.; Jin, R.; Ren, P.; Fang, Y.; Zhang, R.; Wang, Z.-j. Boosting CO2 hydrogenation to methanol by adding trace amount of Au into Cu/ZnO catalysts. *Applied Catalysis B: Environmental* **2023**, *324*, 122233.
(7) Snider, J. L.; Streibel, V.; Hubert, M. A.; Choksi, T. S.; Valle, E.; Upham, D. C.; Schumann, J.; Duyar, M. S.; Gallo, A.; Abild-Pedersen, F. Revealing the synergy between oxide and alloy phases on the performance of bimetallic In–Pd catalysts for CO2 hydrogenation to methanol. *Acs Catalysis* **2019**, *9* (4), 3399-3412.
(8) Zhu, J.; Cannizzaro, F.; Liu, L.; Zhang, H.; Kosinov, N.; Filot, I. A.; Rabeah, J.; Brückner, A.; Hensen, E. J. Ni–In synergy in CO2 hydrogenation to methanol. *ACS catalysis* **2021**, *11* (18), 11371-11384.
(9) Jiang, F.; Wang, S.; Liu, B.; Liu, J.; Wang, L.; Xiao, Y.; Xu, Y.; Liu, X. Insights into the influence of CeO2 crystal facet on CO2 hydrogenation to methanol over Pd/CeO2 catalysts. *ACS Catalysis* **2020**, *10* (19), 11493-11509.
(10) Bahruji, H.; Bowker, M.; Hutchings, G.; Dimitratos, N.; Wells, P.; Gibson, E.; Jones, W.; Brookes, C.; Morgan, D.; Lalev, G. Pd/ZnO catalysts for direct CO2 hydrogenation to methanol. *Journal of catalysis* **2016**, *343*, 133-146.
(11) Frei, M. S.; Mondelli, C.; García-Muelas, R.; Kley, K. S.; Puértolas, B.; López, N.; Safonova, O. V.; Stewart, J. A.; Curulla Ferré, D.; Pérez-Ramírez, J. Atomic-scale engineering of indium oxide promotion by palladium for methanol production via CO2 hydrogenation. *Nature communications* **2019**, *10* (1), 3377.
(12) Rui, N.; Wang, Z.; Sun, K.; Ye, J.; Ge, Q.; Liu, C.-j. CO2 hydrogenation to methanol over Pd/In2O3: effects of Pd and oxygen vacancy. *Applied Catalysis B: Environmental* **2017**, *218*, 488-497.
(13) Lee, K.; Anjum, U.; Araújo, T. P.; Mondelli, C.; He, Q.; Furukawa, S.; Pérez-Ramírez, J.; Kozlov, S. M.; Yan, N. Atomic Pd-promoted ZnZrOx solid solution catalyst for CO2 hydrogenation to methanol. *Applied Catalysis B: Environmental* **2022**, *304*, 120994.
(14) Nie, X.; Jiang, X.; Wang, H.; Luo, W.; Janik, M. J.; Chen, Y.; Guo, X.; Song, C. Mechanistic understanding of alloy effect and water promotion for Pd-Cu bimetallic catalysts in CO2 hydrogenation to methanol. *ACS Catalysis* **2018**, *8* (6), 4873-4892.
(15) Sun, K.; Shen, C.; Zou, R.; Liu, C.-j. Highly active Pt/In2O3-ZrO2 catalyst for CO2 hydrogenation to methanol with enhanced CO tolerance: The effects of ZrO2. *Applied*

Catalysis B: Environmental **2023**, *320*, 122018.
(16) Shen, C.; Sun, K.; Zou, R.; Wu, Q.; Mei, D.; Liu, C.-j. CO2 hydrogenation to methanol on indium oxide-supported rhenium catalysts: the effects of size. *ACS Catalysis* **2022**, *12* (20), 12658-12669.
(17) Manto, M. J.; Xie, P.; Wang, C. Catalytic Dephosphorylation Using Ceria Nanocrystals. *ACS Catalysis* **2017**, *7* (3), 1931-1938.
(18) Wang, W.; Qu, Z.; Song, L.; Fu, Q. CO2 hydrogenation to methanol over Cu/CeO2 and Cu/ZrO2 catalysts: Tuning methanol selectivity via metal-support interaction. *Journal of Energy Chemistry* **2020**, *40*, 22–30.